J|A|C|S

A R T I C L E S

Long Tethers Binding Redox Centers to Polymer Backbones Enhance Electron Transport in Enzyme "Wiring" Hydrogels

Fei Mao,[†] Nicolas Mano,[‡] and Adam Heller*,[‡]

Contribution from TheraSense Inc., 1360 South Loop Road, Alameda, California 94502, and Department of Chemical Engineering and Texas Materials Institute, The University of Texas at Austin, Austin, Texas 78712

Received November 27, 2002; Revised Manuscript Received February 24, 2003; E-mail: Email: heller@che.utexas.edu

Abstract: A redox hydrogel with an apparent electron diffusion coefficient (D_{app}) of $(5.8 \pm 0.5) \times 10^{-6}$ cm^2 s^{-1} is described. The order of magnitude increase in D_{app} relative to previously studied redox hydrogels results from the tethering of redox centers to the backbone of the cross-linked redox polymer backbone through 13 atom spacer arms. The long and flexible tethers allow the redox centers to sweep electrons from large-volume elements and to collect electrons of glucose oxidase efficiently. The spacer arms make the collection of electrons from glucose oxidase so efficient that glucose is electrooxidized already at -0.36 V versus Ag/AgCl, the reversible potential of the redox potential of the FAD/FADH$_2$ centers of the enzyme at pH 7.2. The limiting current density of 1.15 mA cm^{-2} is reached at a potential as low as -0.1 V versus Ag/AgCl. The novel redox center of the polymer is a tris-dialkylated N,N'-biimidazole Os$^{2+/3+}$ complex. Its redox potential, -0.195 V versus Ag/AgCl, is 0.8 V reducing relative to that of Os(bpy)$^{2+/3+}$, its 2,2′-bipyridine analogue.

Introduction

The conduction of electrons in redox polymers has been the subject of studies spanning three decades.[1,2] Electrons are transported in redox polymers by hopping between immobile redox centers, by collisions of mobile reduced and oxidized redox centers, and in some through conjugated and conductive backbones.[3–6] In the absence of conjugation and unless the polymer is so heavily loaded with redox centers that hopping is rapid, the dominant cause of conduction is collisional electron transfer between reduced and oxidized redox centers tethered to the polymer backbone. Because the rate of electron-transferring collisions increases with the mobility of the tethered redox centers, the greater the segmental mobility of the polymer, the faster the electrons diffuse.[7] The segmental mobilities increase upon solvation of the polymer, decrease upon its cross-linking, and are reduced by attractive Coulombic, hydrogen-bonding, dipolar, or induced-dipolar interactions between segments, which raise the glass transition temperatures of polymers.

The transport of electrons through redox polymers is measured by their apparent electron diffusion coefficients, D_{app}. Variations in the controlling parameters have led to redox polymers with D_{app} values as low as 10^{-12} cm^2 s^{-1} and as large as 10^{-6} cm^2 s^{-1}. The coefficient can be determined by electrochemical impedance spectroscopy,[8,9] by measuring the transient currents passing through the polymer-coated electrodes when the potential is stepped[4,10–19] or by measuring the steady-state currents using interdigitated microelectrode arrays (IDAs).[4,20–26] While the IDA-measured D_{app} is independent of the diffusion coefficient of the mobile counterions, it depends on the microscopic counterion displacement associated with the reduction or oxidation of a particular redox center,[27,28] the subject of theoretical studies of Dahms,[29] Laviron,[30] Andrieux,[31]

† TheraSense In.
‡ The University of Texas at Austin.

(1) Murray, R. W. In *Electroanalytical Chemistry*; Bard, A. J., Ed.; Dekker: New York, 1984; Vol. 13, pp 191−368.
(2) Willner, I.; Katz, E. *Angew. Chem., Int. Ed.* **2000**, *39*, 1180−1218.
(3) Aoki, A.; Heller, A. *J. Phys. Chem.* **1993**, *97*, 11014−11019.
(4) Rajagopalan, R.; Aoki, A.; Heller, A. *J. Phys. Chem.* **1996**, *100*, 3719−3727.
(5) Heller, A. *Acc. Chem. Res.* **1990**, *23*, 128−134.
(6) Heller, A. *J. Phys. Chem. B* **1992**, *96*, 3579−3587.
(7) Rajagopalan, R.; Heller, A. In *Molecular Electronics: a chemistry for the 21st century monograph*; Jortner, J., Ratner, M., Eds.; Blackwell Science Ltd.: Oxford, U.K., 1997; pp 241−254.

(8) Cameron, C. G.; Pickup, P. G. *J. Am. Chem. Soc.* **1999**, *121*, 11773−11779.
(9) Cameron, C. G.; Pittman, T. J.; Pickup, P. G. *J. Phys. Chem. B* **2001**, *105*, 8838−8844.
(10) Daum, P. H.; McHalsky, M. L. *Anal. Chem.* **1980**, *52*, 340−344.
(11) Daum, P. H.; Murray, R. W. *J. Phys. Chem.* **1981**, *85*, 389−396.
(12) Gregg, B. A.; Heller, A. *J. Phys. Chem.* **1991**, *95*, 5970−5975.
(13) Gregg, B. A.; Heller, A. *J. Phys. Chem.* **1991**, *95*, 5976−5980.
(14) De Lumley-Woodyear, T.; Rocca, P.; Lindsay, J.; Dror, Y.; Freeman, A.; Heller, A. *Anal. Chem.* **1995**, *67*, 1332−1337.
(15) Forster, R. J.; Vos, J. G.; Lyons, M. E. G. *J. Chem. Soc., Faraday Trans.* **1991**, *87*, 3769−3774.
(16) Forster, R. J.; Vos, J. G.; Lyons, M. E. G. *J. Chem. Soc., Faraday Trans.* **1991**, *87*, 3761−3770.
(17) Forster, R. J.; Vos, J. G. *J. Electrochem. Soc.* **1992**, *139*, 1503−1509.
(18) Oh, S.-M.; Faulkner, L. R. *J. Am. Chem. Soc.* **1989**, *111*, 5613−5618.
(19) Oh, S.-M.; Faulkner, L. R. *J. Electroanal. Chem.* **1989**, *269*, 77−97.
(20) Goss, C. A.; Majda, M. *J. Electroanal. Chem.* **1991**, *300*, 377−385.
(21) Chidsey, C. E.; Feldman, B. J.; Lundgren, C.; Murray, R. W. *Anal. Chem.* **1986**, *58*, 601−607.
(22) Feldman, B. J.; Murray, R. W. *Anal. Chem.* **1986**, *58*, 5844−5847.
(23) Feldman, B. J.; Murray, R. W. *Inorg. Chem.* **1987**, *26*, 1702−1708.
(24) Dalton, E. F.; Surridge, N. A.; Jernigan, J. C.; Wilbourn, K. O.; Facci, J. S.; Murray, R. W. *Chem. Phys.* **1990**, *140*, 143−157.
(25) Nishihara, H.; Dalton, F.; Murray, R. W. *Anal. Chem.* **1991**, *63*, 2955−2960.
(26) Aoki, A.; Rajagopalan, R.; Heller, A. *J. Phys. Chem.* **1995**, *99*, 5102−5110.
(27) Saveant, J.-M. *J. Electroanal. Chem.* **1988**, *242*, 1−21.
(28) Saveant, J.-M. *J. Electroanal. Chem.* **1987**, *238*, 1−8.

Ruff,[32,33] and Buck.[34,35] In conjugated redox polymers based on the complexation of poly(2-(2-bipyridyl)bibenzimidazole) with bis(2,2′-bipyridyl) Ru^{2+} or bis(2,2′-bipyridyl) Os^{2+}, Cameron and co-workers reported $D_{app} \approx 10^{-8}$ cm^2 s^{-1} in acetonitrile with 0.1 M Et$_4$NClO$_4$.[8,9] For the conjugated nonredox polymers polypyrrole and poly(1-methyl-3-pyrrol-1-methylpyridinium), Mao and Pickup reported $D_{app} \approx 10^{-8}$ cm^2 s^{-1}.[36] The two highest D_{app} values, 1.7×10^{-6} and 6×10^{-5} cm^2 s^{-1} were reported by Murray and co-workers,[37,38] respectively, for poly-[Os(bpy)$_2$(vpy)$_2$] sandwiched between a Pt and a porous Au electrode bathed in dry N$_2$ and for doped poly(benzimidazo-benzophenanthroline).

Redox hydrogels constitute the only electron-conducting matrixes in which both the permeation of water-soluble biological reactants and products and the transport of electrons are rapid. They are particularly relevant to electrochemical biosensors and biofuel cells,[6,39–48] in which redox hydrogels electrically "wire" reaction centers of coimmobilized enzymes to electrodes. The absence of leachable components from the "wired" enzyme electrodes allows their use in the body, in flow cells, and in miniature, compartmentless biofuel cells, exemplified by the glucose−O$_2$ cell, in which glucose is electrooxidized to gluconolactone, while O$_2$ is electroreduced to water. The reported values of D_{app} in redox hydrogels in equilibrium with aqueous solutions range between 10^{-12} and 10^{-7} cm^2 s^{-1}.[40,44] Forster and co-workers systematically investigated electron transport in redox hydrogel films,[49–52] exemplified by poly(4-vinylpyridine) with part of the pyridines coordinated with [Os(bpy)$_2$Cl]$^{+/2+}$.[15,16,53,54] D_{app}, typically of ∼10^{-9} cm^2 s^{-1} [51] in H$_2$SO$_4$ and in 1 M NaCl,[49,53] depended on the nature of the electrolyte and its concentration, the temperature, and the loading of redox centers. Sirkar and Pishko[55] reported a D_{app} value as low as 2×10^{-12} cm^2 s^{-1} for a hydrogel based on the copolymer of poly(ethylene glycol) diacrylate and vinylferrocene in a phosphate buffer solution. Komura et al.[56] reported D_{app}∼2 ×

10^{-10} cm^2 s^{-1} for the conjugated nonredox polymer poly(N,N'-bis(3-pyrrol-1-yl-propyl)-4,4′-bipyridinium) chloride in aqueous 0.2 M NaCl. Bu and co-workers[57] reported D_{app} values between 6×10^{-8} and 6×10^{-7} cm^2 s^{-1} for redox hydrogels made by copolymerizing vinylferrocene, acrylamide, and N,N'-methyl-enebisacrylamide.

Blauch and Saveant[58,59] developed a bounded diffusion model to predict D_{app} for polymers when the displacement of the redox centers is rapid and extensive. According to the model

$$D_{app} = {}^1\!/_6 k_{ex}(\delta^2 + 3\lambda^2)C_{RT} \qquad (1)$$

where k_{ex} is the solution-phase self-exchange rate of the redox species, δ is the characteristic electron hopping distance, λ is the distance across which the tethered redox center can actually move, and C_{RT} is the concentration of the redox species. The model suggested that D_{app} could scale in redox hydrogels[4,7] with the square of the length of the tethers. Here we describe the synthesis, characteristics, and application of a redox hydrogel with a particularly high D_{app}. Its redox polymer differs from earlier redox polymers by having 13-atom-long tethers between the redox centers and the polymer backbone. When the hydrogel swells, the tethers and their terminal cationic redox center become mobile, sweeping large volume elements. They collect electrons from redox centers of coimmobilized glucose oxidase efficiently already at highly reducing potentials.

Experimental Section

Synthesis of PVP-[Os(N,N'-dialkylated-2,2′-biimidazole)$_3$]$^{2+/3+}$. The synthesis of polymer **I** is outlined in Scheme 1 and its details are provided as Supporting Information. 2,2′-Biimidazole[60] was bismethylated in DMF with methyl iodide in the presence of sodium hydride, and the resulting N,N'-dimethyl-2,2′-biimidazole (DMB) was purified by sublimation. To introduce the 13-atom-long flexible tether, the primary amine of the N-(6-aminohexyl)-N'-methyl-2,2′-biimidazole (AMB) ligand was condensed with the alkylidene carboxylate attached to the backbone of the polymer, as described below. AMB was synthesized in three steps: In the first, 2,2′-biimidazole was methylated with 1 equiv of methyl iodide, the reaction yielding a mixture of mono- and dimethylbiimidazole and unreacted 2,2′-biimidazole. The desired monomethylbiimidazole, was, however, the major product and was readily isolated by recrystallization from EtOAc/hexane. In the second step, the monomethylbiimidazole was alkylated with N-(6-bromohexyl)-phthalimide plus sodium hydride, with sodium iodide activating the bromoalkyl compound. In the third step, the ligand, in which the primary amine was still protected, was deprotected by hydrazine in refluxing ethanol. After silica gel column chromatography with NH$_4$OH/CH$_3$CN, the yield of AMB was 50%.

The primary amine-containing osmium complex was synthesized in a one-pot reaction. Heating of 2 equiv of DMB and 1 equiv of NH$_4$OsCl$_6$ (or K$_2$OsCl$_6$) in ethylene glycol under nitrogen yielded the [Os^{III}(DMB)$_2$Cl$_2$]Cl intermediate, which, without isolation, was directly reacted with 1 equiv of AMB to give the desired complex [Os^{II}(DMB)$_2$-(AMB)](Cl)$_2$. The complex was readily air oxidized, its green color changing to blue as the [Os^{III}(DMB)$_2$(AMB)](Cl)$_2$ formed. To convert the dichloride to DMF-soluble [Os^{III}(DMB)$_2$(AMB)](PF$_6$)$_3$, the aqueous solution of [Os^{II}(DMB)$_2$(AMB)](Cl)$_2$ was stirred with beads of the

(29) Dahms, H. *J. Phys. Chem.* **1968**, *72*, 362.
(30) Laviron, E. J. *J. Electroanal. Chem.* **1980**, *112*, 1.
(31) Andrieux, C. P.; Saveant, J.-M. *J. Electroanal. Chem.* **1980**, *111*, 377.
(32) Ruff, I.; Friedrich, V. J. *J. Phys. Chem.* **1971**, *75*, 3297.
(33) Ruff, I.; Friedrich, V. J.; Demeter, K.; Csillag, K. *J. Phys. Chem.* **1971**, *75*, 3303.
(34) Buck, R. P. *J. Electroanal. Chem.* **1988**, *243*, 279.
(35) Buck, R. P. *J. Phys. Chem.* **1983**, *87*, 279.
(36) Mao, H.; Pickup, P. G. *J. Am. Chem. Soc.* **1990**, *112*, 1776−1782.
(37) Jernigan, J. C.; Murray, R. W. *J. Am. Chem. Soc.* **1987**, *109*, 1738−1745.
(38) Wilbourn, K.; Murray, R. W. *J. Phys. Chem.* **1988**, *92*, 3642−3648.
(39) Katz, E.; Buckmann, A. F.; Willner, I. *J. Am. Chem. Soc.* **2001**, *123*, 10752−10753.
(40) Mano, N.; Mao, F.; Heller, A. *J. Am. Chem. Soc.* **2002**, *124*, 12962−12963.
(41) Chen, T.; Barton, S. C.; Binyamin, G.; Gao, Z.; Zhang, Y.; Kim, H.-H.; Heller, A. *J. Am. Chem. Soc.* **2001**, *123*, 8630−8631.
(42) Mano, N.; Kim, H.-H.; Heller, A. *J. Phys. Chem. B* **2002**, *106*, 8842−8848.
(43) Mano, N.; Kim, H.-H.; Zhang, Y.; Heller, A. *J. Am. Chem. Soc.* **2002**, *124*, 6480−6486.
(44) Kim, H.-H.; Mano, N.; Zhang, Y.; Heller, A. *J. Electrochem. Soc.* **2003**, *150*, A209−A213.
(45) Ohara, T. J.; Rajagopalan, R.; Heller, A. *Anal. Chem.* **1993**, *65*, 3512−3517.
(46) Baldini, E.; Dall'Orto, V. C.; Danilowicz, C.; Rezzano, I.; Calvo, E. J. *Electroanalysis* **2002**, *14*, 1157−1164.
(47) Vreeke, M.; Maidan, R.; Heller, A. *Anal. Chem.* **1992**, *64*, 3084−3090.
(48) Ohara, T. J.; Rajagopalan, R.; Heller, A. *Anal. Chem.* **1994**, *66*, 2451−2457.
(49) Forster, R. J.; Kelly, A. J.; Vos, J. G.; Lyons, M. E. G. *J. Electroanal. Chem.* **1989**, *270*, 365−379.
(50) Forster, R. J.; Vos, J. G. *J. Chem. Soc., Faraday Trans.* **1991**, *87*, 1863−1868.
(51) Forster, R. J.; Vos, J. G. *J. Electroanal. Chem.* **1991**, *314*, 135−152.
(52) Keane, L.; Hogan, C.; Forster, R. J. *Langmuir* **2002**, *18*, 4826−4833.
(53) Forster, R. J.; Vos, J. G. *Electrochim. Acta* **1992**, *37*, 159−167.
(54) Forster, R. J.; Vos, J. G. *Langmuir* **1994**, *10*, 4330−4338.
(55) Sirkar, K.; Pishko, M. V. *Anal. Chem.* **1998**, *70*, 2888−2894.

(56) Komura, T.; Kijima, K.; Yamaguchi, T.; Takahashi, K. *J. Electroanal. Chem.* **2000**, *468*, 166−174.
(57) Bu, H.-Z.; English, A. M.; Mikkelsen, S. R. *J. Phys. Chem. B* **1997**, *101*, 9593−9599.
(58) Blauch, D. N.; Saveant, J.-M. *J. Phys. Chem.* **1993**, *97*, 6444−6448.
(59) Blauch, D. N.; Saveant, J.-M. *J. Am. Chem. Soc.* **1992**, *114*, 3323−3332.
(60) Fieselmann, B. F.; Hendrickson, D. N.; Stucky, G. D. *Inorg. Chem.* **1978**, *17*, 2078.

Scheme 1. Synthetic Route to Polymer **I**, the Chloride of PVP-[Os(*N,N'*-dialkylated-2,2'-biimidazole)₃]²⁺/³⁺*a*
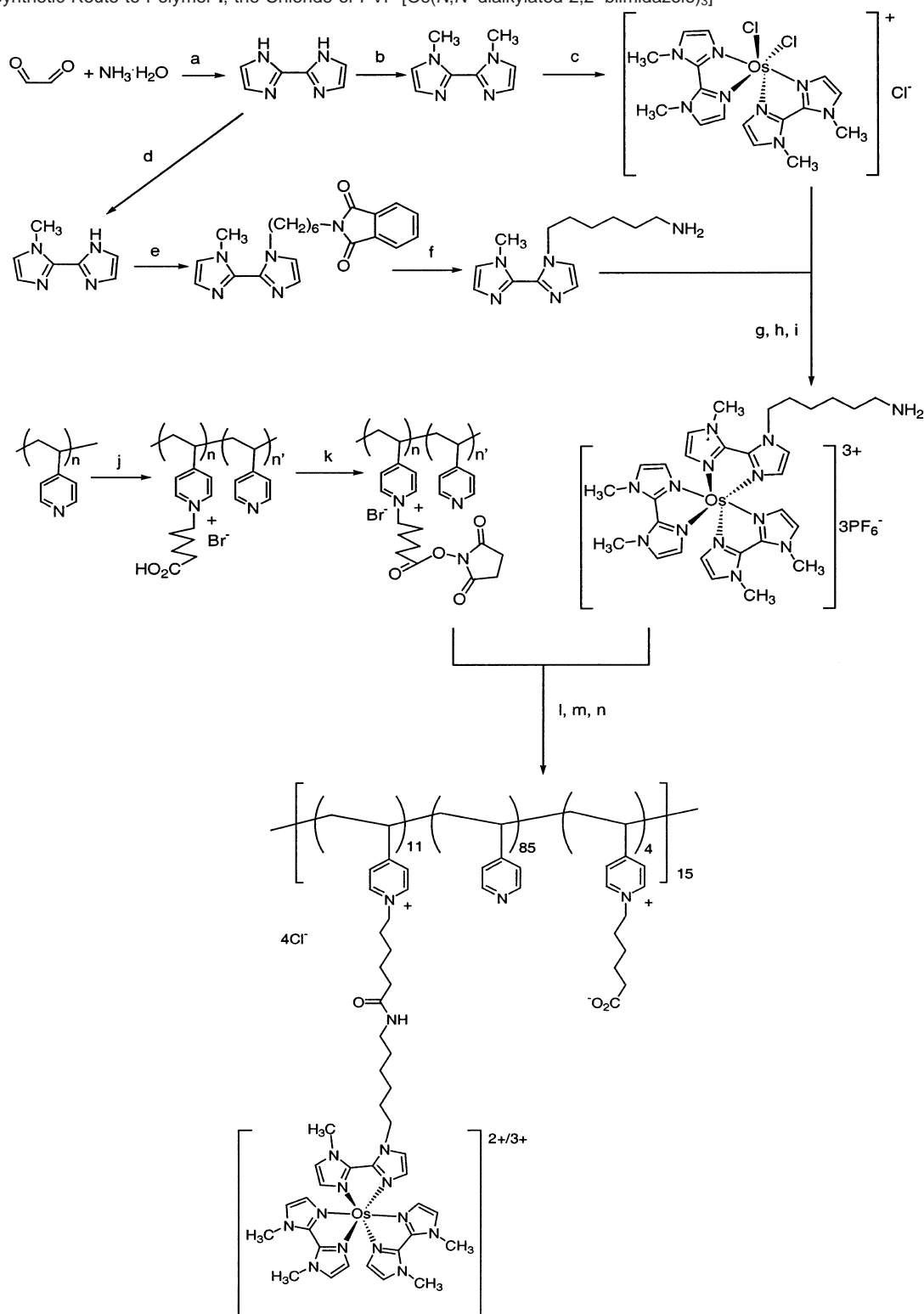
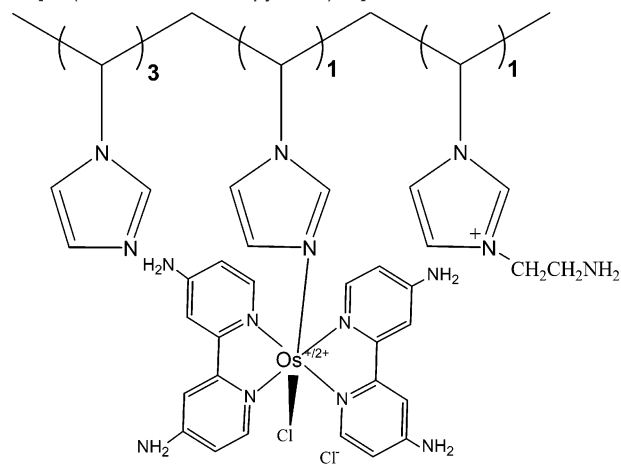*a* Reagents and Conditions: (a) H₂O, 40−50 °C, 24 h; (b) NaH/methyl *p*-toleunesulfonate, DMF, 0 °C to room temperature, 4 h; (c) 0.5 equiv of (NH₄)₂OsCl₆, ethylene glycol, 140 °C, 24 h; (d) 1.1 equiv of NaH/1.0 equiv of CH₃I, DMF, 0 °C to room temperautre, overnight; (e) NaH/*N*-(6-bromohexyl)phthalimide/ NaI, DMF, 80 °C, 24 h; (f) H₂NNH₂, EtOH, reflux, 24 h; (g) ethylene glycol, 140 °C, 24 h; (h) chloride resin/H₂O/air, 24 h; (i) NH₄PF₆/H₂O; (j) 6-bromohexanoic acid/DMF, 90 °C, 24 h; (k) TSTU/*N,N*-diisopropylethylamine, DMF, 7∼8 h; (l) *N,N*-diisopropylethylamine, DMF, room temperature, 24 h; (m) chloride resin/H₂O, 24 h; (n) ultrafiltration.

chloride form of Bio-Rad AG1 × 4 anion-exchange resin, air-oxidized, and then stirred with an excess of NH₄PF₆ to precipitate the air- and humidity-stable [Os^III(DMB)₂(AMB)](PF₆)₃ in high yield.

Poly(4-vinylpyridine) (PVP; MW ∼160 000) was quaternized with 1 equiv of 6-bromohexanoic/∼6 mers of vinylpyridine. The ratio and the quantitative quaternization were confirmed by ¹H NMR. The reactive *N*-hydroxysuccinimidyl ester of the (4-(*N*-(5-carboxypentyl)-pyridinium)-*co*-4-vinylpyridine) polymer was formed in DMF by reacting the polymer with *O*-(*N*-succinimidyl)-*N,N,N',N'*-tetramethyl-uronium tetrafluoroborate (TSTU) and a base. The NHS ester of the

Chart 1. Structure of Polymer **II**,
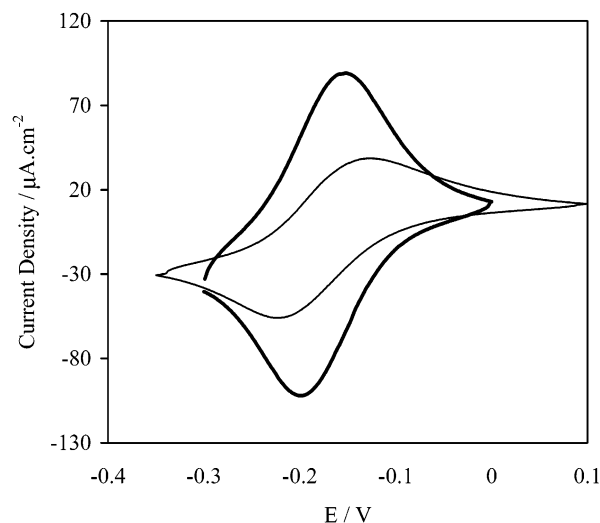PVI-[Os(4,4′-diamino-2,2′bipyridine)₂Cl] $^{+/2+}$

Figure 1. Cyclic voltammograms of adsorbed, non-cross-linked thin films of polymers **I** (heavy line) and **II** (fine line) on a 3-mm-diameter glassy carbon electrode under argon: 0.1 M NaCl, 20 mM phosphate buffer pH 7, 37 °C, 20 mV/s. Potentials versus that of the Ag/AgCl (3M KCl) reference electrode.

polymer was not isolated but directly reacted at room temperature while still in the DMF solution with a 1.3-fold excess of Os^{III}(DMB)₂(AMB)]-(PF₆)₃ to form the PF₆⁻ salt of the desired blue redox polycation **I**. The PF₆⁻ salt of the polymer was soluble in polar organic solvents such as CH₃CN and DMF but was insoluble in water. To convert it to the water soluble polymer, the PF₆⁻ was Cl⁻ exchanged using the chloride of the AG1 × 4 resin. The polymer was characterized by measuring its Os, C, and N content and its NMR spectrum. These showed that 70% of the *N*-(5-carboxypentyl)pyridinium functions reacted to form the amide with the osmium complex. The (tethered complex)/pyridine/(carboxypentylpyridinium) ratio was 10.6:85:4.4.

Other Chemicals and Materials. Ultrapure argon was purchased from Matheson (Austin, TX). K₂OsCl₆ was purchased from Alpha Chemicals, *N*-(6-bromohexyl)phthalimide from Lancaster, and AG1 × 4 chloride resin from Bio-Rad Laboratories (Hercules, CA). Glucose oxidase from *Aspergillus niger* was purchased from Fluka (Milwaukee, MI). The other chemicals were purchased from Aldrich Chemicals (St. Louis, MO). The electrochemical measurements were performed in pH 7.4 20 mM phosphate-buffered 0.15 M NaCl (PBS). The solutions were made with water deionized in a purification train (Sybron Chemicals Inc, Pittsburgh, PA). Poly(ethylene glycol) (400) diglycidyl ether (PEGDGE) was purchased from Polysciences Inc., Warrington, PA. The synthesis of redox polymer **II** PVI-[Os(4,4′-diamino-2,2′-bipyridine)₂Cl]$^{+/2+}$, shown in Chart 1, was previously reported.[44]

Instrumentation and Analysis. ¹H NMR spectra were obtained on a JEOL 400 or a Nicolet/GE NT300 NMR spectrometer by Acorn NMR, Inc. (Livermore, CA) and elemental analyses were performed by Quantitative Technologies, Inc. (Whitehouse, NJ). Both cyclic voltammetry and double-step chronoamperometry were performed using a bipotentiostat (CH−Instruments, Electrochemical Detector model CHI832) and a dedicated computer. In the chronoamperometric experiments, the potential was stepped between −0.4 and +1.2 V versus Ag/AgCl and 20 measurements were averaged. The contribution from the capacitive background was estimated by stepping the potential from +0.1 to 1.2 V, where no Faradaic reaction occurred. After extrapolation, this capacitive component was subtracted from the total current measured for the Faradaic reaction. Surface coverages of the modified electrodes were determined by integration of the voltammetric waves of the redox polymer films at 1 mV/s, assuming that the geometrical area of the polished 3-mm-diameter glassy carbon electrodes was their true area.

The measurements were carried out in a water-jacketed electrochemical cell containing 50 mL of PBS at 37.5 °C. To maintain a fixed volume of solution, the bubbled gases were presaturated with water. The potentials were measured versus a Ag/AgCl (3 M KCl) reference electrode. The counter electrode was a platinum wire (BAS, West Lafayette, IN).

The thicknesses of the dry and swollen redox polymer films were obtained from backscattered electron micrographs, produced by an environmental scanning electron microscope (ESEM).[26] The imaged film consisted of 91 wt % polymer and 9 wt % cross-linker. After the film was deposited on the polished side of silicon wafers, it was cured at room temperature for >24 h. The wafer was then cleaved to allow cross sectional imaging of the polymers film.

Electrodes. Vitreous carbon rotating disk electrodes (V-10 grade from Atomergic (Farmingdale, NY) of 3-mm diameter were prepared as previously reported.[12,13] They were polished sequentially with slurries of 5-, 1-, and 0.3-μm alumina particles (Buehler, Lake Bluff, IL), sonicated, and rinsed with ultrapure water. The cleaning process was repeated until no voltammetric features were observed between the potentials of interest (−0.4 to 0.4 V vs Ag/AgCl) in 50 mV/s scans in PBS. The total loaded amount of polymer and cross-linker was constant at 130 μg/cm², with 2 μL of a 4.3 mg/mL polymer/PEDGE solution deposited on the surface. After deposition and drying, the films were cured for at least 18 h at room temperature before the electrodes were used.

Carbon Fiber Electrodes. Prior to their coating, the 7-μm-diameter fibers (0.0044 cm²) were made hydrophilic by exposure to 1 Torr O₂ plasma for 3 min.[61] The anodic catalyst solution was made as follows: 100 μL of 40 mg/mL GOx in 0.1 M NaHCO₃ was oxidized by 50 μL of 7 mg/mL NaIO₄ in the dark for 1 h, and then 2 μL of the periodate-oxidized GOx was mixed with 8 μL of a 10 mg/mL concentration of the chloride of polymer **II** or of polymer **I** and a 0.5-μL droplet of 2.5 mg/mL PEGDGE. A 5-μL aliquot of this solution was applied to the fiber. The resulting electrocatalyst consisted of the cross-linked adduct of 39.6 wt % GOx, 59.5 wt % redox polymer, and 0.9 wt % PEDGE.

Results and Discussion

Polymer **I**, PVP-[Os(*N*,*N*′-dialkylated-2,2′-bi-imidazole)₃)]$^{2+/3+}$, with a 13-atom-long flexible tether, had a novel redox function, a tris-*N*,*N*′-dialkylated 2,2′-biimidazole complex of Os$^{2+/3+}$. Its redox potential, −0.195 V versus Ag/AgCl in a 0.1 M chloride solution (Figure 1) was 0.8 V negative of the familiar analogous tris-2,2′-bipyridine complex of Os$^{2+/3+}$, Os(bpy)₃$^{2+/3+}$. The reference PVI-[Os(diamino-bipyridine)₂Cl]$^{+/2+}$, polymer **II**, without a tether between its redox function and the backbone, had a similar redox potential of −0.185 V versus Ag/AgCl.

(61) Sayka, A.; Eberhart, J. G. *Solid State Technol* **1989**, *32*, 69−70.

Figure 1 shows the cyclic voltammograms of adsorbed but not cross-linked thin films of polymer **I** (heavy line) and polymer **II** (fine line) under argon in pH 7, 0.1 M NaCl, 20 mM phosphate buffer at 37 °C. The voltammograms are characteristic of polymer-bound osmium complexes. At 1 mV/s scan rate, polymer **I** exhibited a symmetrical wave, with only slight (5 mV) separation of the oxidation and reduction peaks, while polymer **II** exhibited a separation of 40 mV. At 20 mV/s scan rate, the voltammogram of polymer **I** exhibited a symmetrical wave with 40-mV peak separation, the separation for polymer **II** was >100 mV. Comparison of the peak separations suggested that D_{app} of polymer **I** was considerably higher than that of polymer **II**.
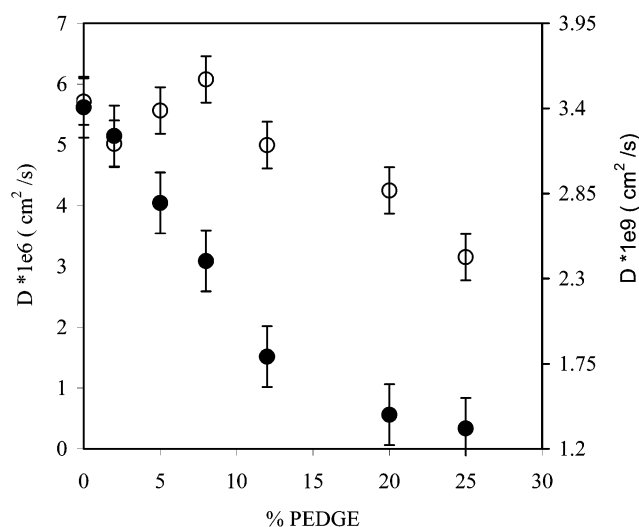
The D_{app} of redox hydrogels depends on the mobility of their tethered redox function; the solution-phase anion, diffusing into and out of the redox polymer when the polymer is oxidized and reduced; and the cross-linking of their polymer, which reduces the mobility of the segments. The products $D_{app}^{1/2}C_{RT}$ were obtained from the cyclic voltammograms by the Randles−Sevcik equation (eq 2),[52,62] by plotting the voltammetric peak

$$i_p = 0.4463nF^{3/2}AD_{app}^{1/2}C_{RT}\nu^{1/2}/(RT)^{1/2} \qquad (2)$$

currents (i_p) versus the square root of the scan rates ($\nu^{1/2}$). In eq 2, n is the number of electrons transferred, F is the Faraday's constant, R is the gas constant, T is the temperature, A is the area of the electrode, and C_{RT} is the effective electroactive site concentration.[44,63] C_{RT} in the hydrated film was calculated from the weight of polymer loaded per unit area and from its swelling, determined by cross sectional ESEM imaging. The images in Figure 6A and B are cross sectional electron micrographs of dry and hydrated films, respectively, of the cross-linked polymer **I**. As seen, the polymer swells upon hydration in PBS to 3.4 times its initial thickness (∼60 μm dry vs ∼200 μm hydrated). As seen in the images of Figure 7, polymer **II** swells upon its hydration much less, only by 60% (∼70 μm dry vs ∼120 μm hydrated). The polymer loadings on all electrodes were fixed at 130 μg/mL, an amount that would yield a 1.3-μm-thick dry and a 4.4-μm-thick hydrated film for polymer **I** and a 1.3-μm-thick dry and a 2.2-μm-thick hydrated film for polymer **II**, for an assumed density of 1 g/cm³.[14] The resulting estimate of D_{app} is $(5.8 \pm 0.5) \times 10^{-6}$ cm² s⁻¹ for polymer **I** and (3.4 ± 0.4) 10^{-9} cm² s⁻¹ for polymer **II**. D_{app} of polymer **I** was measured also by double-potential stepped chronoamperometry,[63] with a large-amplitude potential step applied to avoid the effect of the iR drop across the polymer film,[1,64,65] by plotting i versus $t^{1/2}$ per the Cottrell equation (eq 3).[63] The value obtained was

$$i = nFAD_{app}^{1/2}C_{RT}\pi^{-1/2}t^{1/2} \qquad (3)$$

essentially identical with that obtained by the first method, $(5.2 \pm 0.3) \times 10^{-6}$ cm² s⁻¹. The observed 1700-fold difference in D_{app} is attributed to a 41-fold increase in λ, the physical displacement of the redox centers about their equilibrium positions (eq 1) upon the 13-atom extension of the length their tether.

(62) Forster, R. J.; Vos, J. G. *J. Inorg. Organomet. Polym.* **1991**, *1*, 67−86.
(63) Bard, A. J.; Faulkner, L. R. *Electrochemical Methods. Fundamentals and Applications*; 2nd ed.; John Wiley and Sons: New York, 2001.
(64) Murray, R. W. *Molecular Design of Electrode Surfaces*; Wiley: New York, 1992.
(65) Andrieux, C. P.; Haas, O.; Saveant, J.-M. *J. Am. Chem. Soc.* **1986**, *108*, 8175−8182.

Figure 2. Dependence of D_{app} polymers **II** (open circles, right axis) and polymer **I** (solid circles, left axis) on the weight fraction of the PEGDGE cross-linker. The results obtained were identical when obtained by cyclic voltammetry using the Randles−Sevcik equation and by double-potential stepped chronoamperometry with a large-amplitude potential step applied to avoid effect of the iR drop across the polymer film, by plotting i versus $t^{1/2}$ using the Cottrell equation. Conditions as in Figure 1.

Figure 2 shows the dependence of the D_{app} of polymers **I** (solid circles) and **II** (open circles) on the weight percent of the cross-linker. Each value reported is the average for four double-step chronoamperometric and cyclic voltammetric measurements. Upon increasing the weight percent of the cross-linker from 0 to 25 wt %, the apparent diffusion coefficient of polymer **I** decreased ∼19-fold, from 5.8×10^{-6} cm² s⁻¹ to 0.3×10^{-6} cm² s⁻¹. The apparent diffusion coefficient of polymer **II** did not change significantly with the weight percent of the cross-linker decreasing only from 3.4×10^{-9} cm² s⁻¹ to 2.3×10^{-9} cm² s⁻¹. Figure 3 shows the shifts of the peak potential E_p (open circles, right axis) and peak width at half-height, E_{whm}, (solid circles, left axis) upon increasing the weight percent of the cross-linker. For polymer **I** (Figure 3A), E_{whm} was 90 mV at low (∼2 wt %) cross-linker content, increasing to ∼200 mV at 25 wt %, with E_p increasing from −0.195 to −0.110 V vs Ag/AgCl. Figure 3B shows that E_{whm} for polymer **II** was 120 mV at ∼2 wt % cross-linker, increasing to ∼150 mV at 25 wt %, while E_p shifted from −0.195 to −0.155 V vs Ag/AgCl. Swelling was reduced as the cross-linking of the redox polymer increased. Consistent with the observations of Oh and Faulkner,[18] Bu,[57] and Rajagopalan[4] as the segments became less mobile, D_{app} decreased.
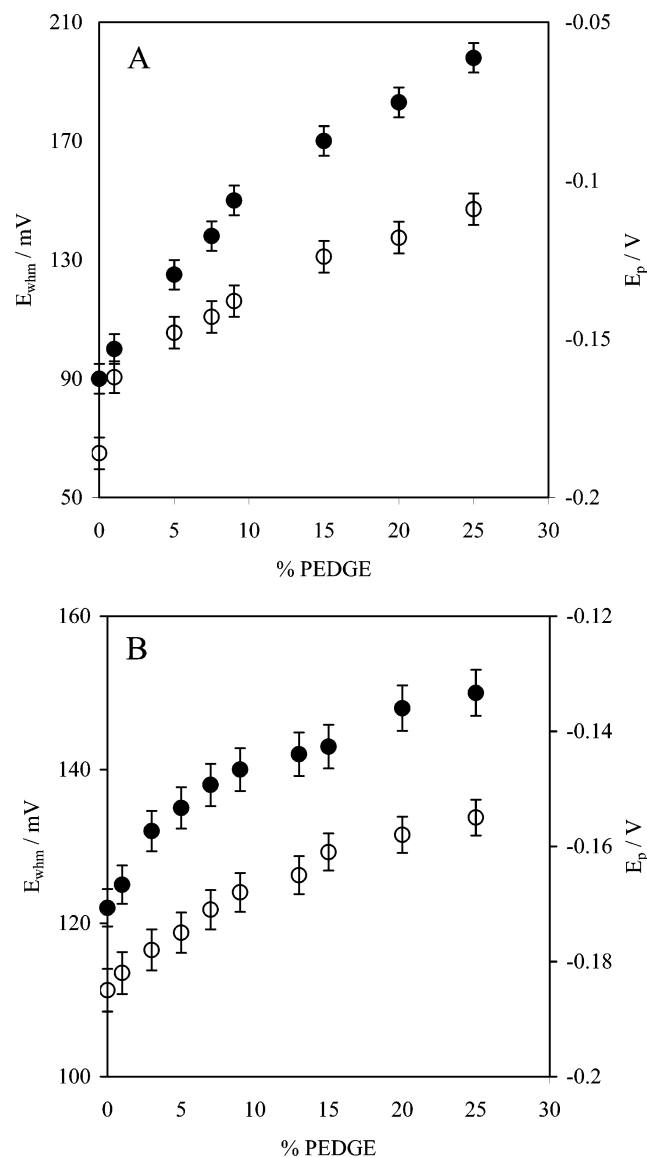
The stability of the integrals of the voltammetric waves of the cross-linked films of polymers **I** and **II** is shown in Figure 4. The films contained 9 wt % of the cross-linker and were cured for 24 h at room temperature. In their stability test, the electrodes were rotated for 20 h at 300 rpm in the pH 7.2, 0.1 M NaCl 20 mM phosphate buffer at 37 °C, while their potential was cycled between −0.4 and +0.1 V versus Ag/AgCl at 50 mV/s. The heights of the voltammetric peaks decreased by 4% for polymer **I** (solid circles) and by 12% for polymer **II** (open circles). Neither the peak potential (ΔE_P) nor the width of the peak at half-height (E_{whm}) changed for either polymer. As seen in the figure, the integral of polymer **I** was considerably more stable than that of polymer **II**. The difference is attributed to the coordinative cross-linking of polymer **II**: upon redox cycling

Figure 3. Dependence of the peak potential E_p (open circles, right axis) and the peak width at half-height, E_{whm} (solid circles, left axis), on the weight fraction of the cross-linker PEGDGE: (A) polymer **I**; (B) polymer **II**. Conditions as in Figure 1.

the inner-sphere chloride of the osmium complex of polymer **II** is exchanged by imidazoles of neighboring chains.[66] The added cross-linking decreases the segmental mobility, the diffusivity of electrons, and thereby the thickness of the electroactive film. Because the complex of polymer **I** does not have an inner-sphere chloride, it is not coordinatively cross-linked and is more stable under redox cycling.

The polarizations of miniature carbon fiber anodes (7 μm diameter, 2 cm long) modified with 39.6 wt % glucose oxidase, 0.9 wt % PEDGE, and 59.5 wt % concentration of either polymer **II** (fine line) or polymer **I** (heavy line) in a quiescent pH 7.2, 0.1 M NaCl, 20 mM phosphate, 15 mM glucose solution under air at 37.5 °C are compared in Figure 5. Glucose was electrooxidized on the fiber with polymer **I** at − 0.1 V versus Ag/AgCl at a current density of 1.15 mA/cm² and the threshold for glucose electrooxidation was −0.36 V versus Ag/AgCl. On the fiber with polymer **II**, the current density at −0.1 V versus Ag/AgCl was only 0.15 mA/cm². The hydrated films of cross-linked polymer **I** constitute the best electron-conducting hy-
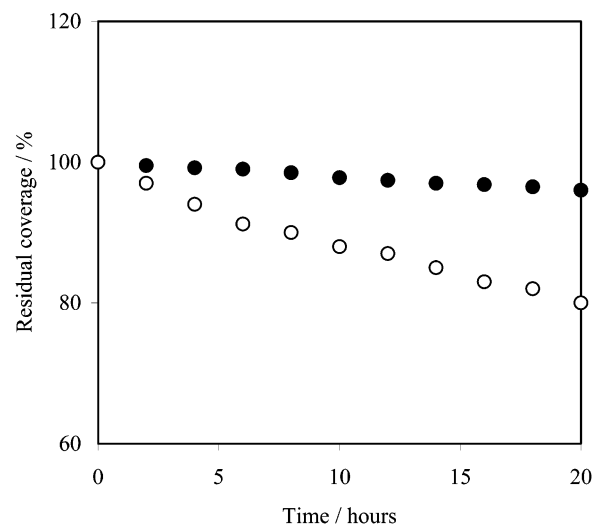
Figure 4. Percent decrease in the integrated voltammetric waves of cross-linked (9 wt % cross-linker) films of polymers **I** (solid circles) and **II** (open circles) upon cycling the applied potential for 20 h between −0.4 and +0.1 V vs Ag/AgCl at 50 mV/s. The loading of the polymers was 130 μg/cm². Electrodes rotating at 300 rpm, pH 7.2, 0.1 M NaCl, 20 mM phosphate buffer; 37 °C.
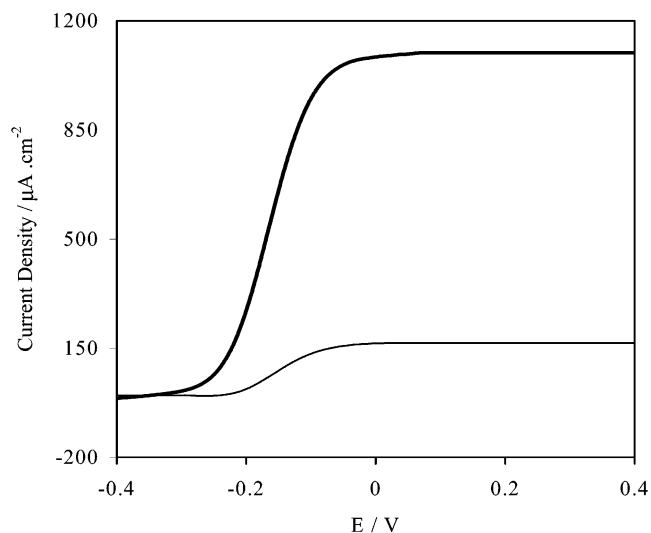

Figure 5. Polarization of 7-μm-diameter, 2-cm-long carbon fiber anode modified with PVI-[Os(4,4′-diamino-2,2′-bipyridine)₂Cl]⁺/²⁺ (fine line) and with PVP-[Os(N,N′-dialkylated-2,2′biimidazole)₃]²⁺/³⁺ (heavy line). Quiescent solution, under air, 37.5 °C, PBS buffer, 15 mM glucose, 1 mV/s.

drogels and the best "wires" of glucose oxidase to date. Even though the redox potential of the hydrogel formed upon cross-linking polymer **I** with PEGDGE is highly reducing, −195 mV versus Ag/AgCl, the polymer efficiently oxidizes the FADH₂ centers of glucose oxidase. The Figure 5 polarization curves of 7-μm-diameter, 2-cm-long carbon fiber anodes made by wiring GOx with polymers **I** and **II** show that the limiting current density of glucose electrooxidation is reached with both polymers already at − 0.1 V versus Ag/AgCl, only 0.26 V positive the redox potential of the FAD/FADH₂ cofactor in GOx at pH 7.2.[67] The limiting current density of electrodes made with polymer **II** is, however, only 0.15 mA/cm², well below the 1.15 mA/cm² limiting current density of the electrode made

(66) Gao, Z.; Binyamin, G.; Kim, H.-H.; Barton, S. C.; Zhang, Z.; Heller, A. *Angew. Chem., Int. Ed.* **2002**, *41*, 810−813.

(67) Stankovich, M. T.; Schopfer, L. M.; Massey, V. *J. Biol. Chem.* **1978**, *253*, 4971−4979.
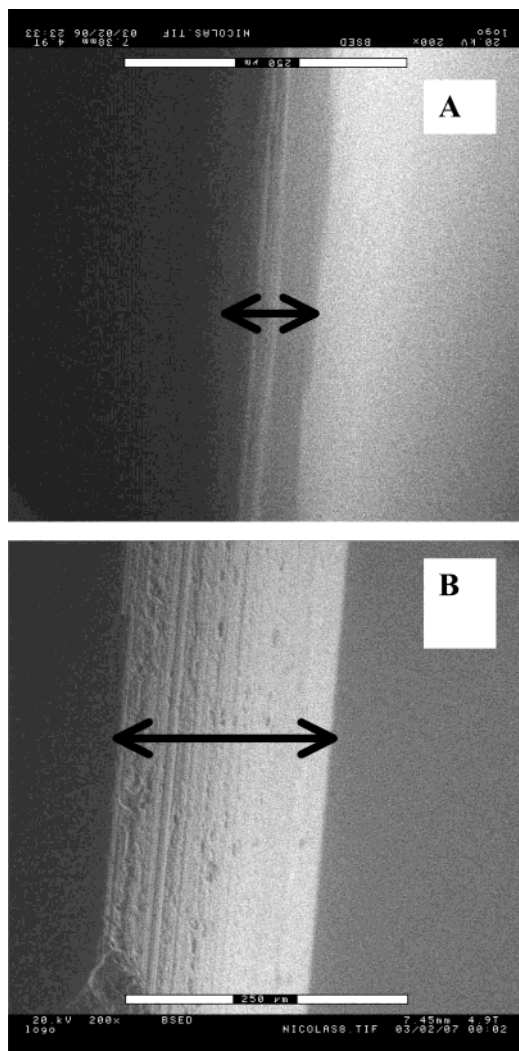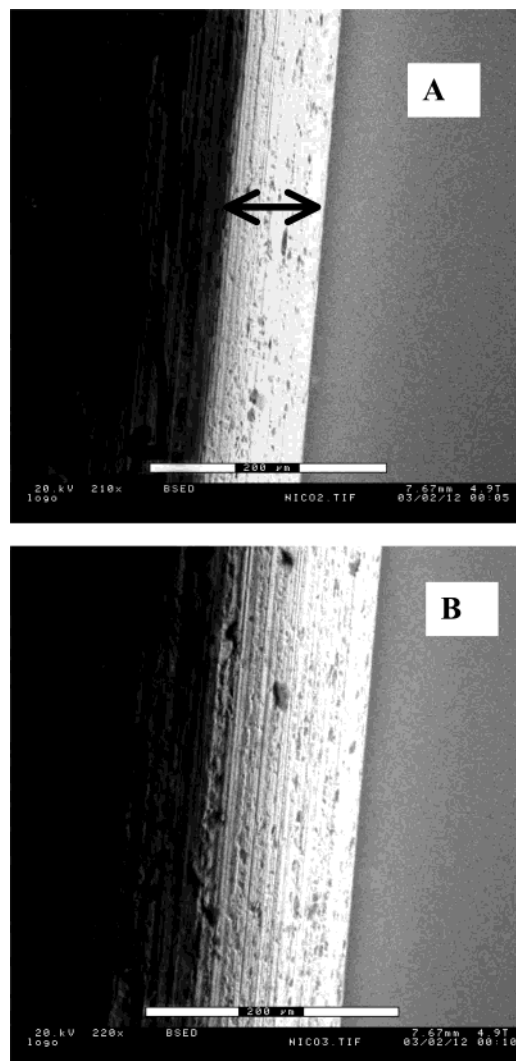
Figure 6. Cross sectional scanning electron micrographs of films of cross-linked polymer **I** on a polished silicon wafer. The images were obtained using backscattered electron detection: (A) image of the dry film; (B) the same film after its hydration. 9 wt % PEDGE. Scale 250 μm, Magnification $\times 200$. Pressure 4.9 T. The dark zones on the left are silicon; the redox polymer films are lighter.

Figure 7. Cross sectional scanning electron micrographs of films of cross-linked polymer **II** on a polished silicon wafer. The images were obtained using backscattered electron detection: (A) image of the dry film; (B) the same film after its hydration. 9 wt % PEDGE. Scale 200 μm. Magnification $\times$ 200. Pressure 4.9 T. The dark zones on the left are silicon; the redox polymer films are lighter.

with polymer **I**. Electrodes made with polymer **I** are the only ones on which the electrooxidation of glucose starts already at the redox potential of the FAD/FADH$_2$ centers of GOx, -360 mV versus Ag/AgCl[67] at pH 7.2. (Figure 5) Thus, the long tethers not only increase the apparent diffusivity of electrons but also facilitate electron transfer from the reduced (FADH$_2$) reaction centers of glucose oxidase to the redox polymer.

Conclusion

The redox potential of the novel tris(*N, N'*-dialkylated 2,2'-biimidazole) Os$^{2+/3+}$ complex, -0.195 V versus Ag/AgCl, is 0.8 V reducing relative to its familiar 2,2'bipyridine analogue, Os(bpy)$_3$$^{2+/3+}$. Like Os(bpy)$_3$$^{2+/3+}$ and its derivatives, the dialkylated bi-imidazole complex is a fast redox couple. Its tethering to the backbone of a polymer through a 13-atom-long flexible spacer and cross-linking and hydration of the resulting polymer yields a hydrogel in which electrons diffuse 1 order of magnitude more rapidly [$D_{app} = (5.8 \pm 0.5) \times 10^{-6}$ cm^2 s^{-1}] than in previously reported hydrogels. When the hydrogel "wires" the FAD/FADH$_2$ centers of glucose oxidase to an electrode, glucose is electrooxidized at pH 7.2 already at -0.36

V versus Ag/AgCl, the redox potential of the enzyme's redox centers.[67] A 1.15 mA/cm^2 limiting current density of glucose electrooxidation is reached at a potential as reducing as -0.1 V versus Ag/AgCl. In combination with a reported cathode, enabling the rapid four-electron electroreduction of molecular oxygen to water under physiological conditions,[42] this glucose anode forms the basis for a compartment-less, miniature glucose/O$_2$ biofuel cell.[40,68]

Supporting Information Available: Additional information as noted in text. This material is available free of charge via the Internet at http://pubs.acs.org.

JA029510E

(68) Mano, N.; Mao, F.; Shin, W.; Chen, T.; Heller, A. *Chem. Commun.* **2003**, 518−519.